A Mutation in Segment I-S6 Alters Slow Inactivation of Sodium Channels

Sho-Ya Wang and Ging Kuo Wang
Department of Biological Sciences, State University of New York at Albany, Albany, New York 12222, and Department of Anesthesia, Harvard Medical School and Brigham and Women's Hospital, Boston, Massachusetts 02115-6195 USA

ABSTRACT Slow inactivation occurs in voltage-gated Na^+ channels when the membrane is depolarized for several seconds, whereas fast inactivation takes place rapidly within a few milliseconds. Unlike fast inactivation, the molecular entity that governs the slow inactivation of Na^+ channels has not been as well defined. Some regions of Na^+ channels, such as μ1-W402C and μ1-T698M, have been reported to affect slow inactivation. A mutation in segment I-S6 of μ1 Na^+ channels, N434A, shifts the voltage dependence of activation and fast inactivation toward the depolarizing direction. The mutant Na^+ current at +50 mV is diminished by 60–80% during repetitive stimulation at 5 Hz, resulting in a profound use-dependent phenomenon. This mutant phenotype is due to the enhancement of slow inactivation, which develops faster than that of wild-type channels (τ = 0.46 ± 0.01 s versus 2.11 ± 0.10 s at +30 mV, n = 9). An oxidant, chloramine-T, abolishes fast inactivation and yet greatly accelerates slow inactivation in both mutant and wild-type channels (τ = 0.21 ± 0.02 s and 0.67 ± 0.05 s, respectively, n = 6). These findings together demonstrate that N434 of μ1 Na^+ channels is also critical for slow inactivation. We propose that this slow form of Na^+ channel inactivation is analogous to the "C-type" inactivation in *Shaker* K^+ channels.

INTRODUCTION

Voltage-gated Na^+ channels are glycoproteins responsible for the firing of action potentials in excitable membranes (Catterall, 1988). Mammalian Na^+ channels consist of one large α-subunit and one or two smaller auxiliary subunits (β_1 and β_2; Isom et al., 1994). The α-subunit protein contains four homologous repeats (I–IV domains), and each repeat consists of six transmembrane segments (S1-S6). These channels are activated upon depolarization and are then inactivated rapidly, with a mean open time of less than 1 ms (Aldrich et al., 1983). Earlier studies suggested that fast inactivation may be governed by an inactivation particle that plugs the channel from the internal side (for a review see Armstrong, 1992). The molecular entity that controls the fast inactivation of Na^+ channels has been delineated recently to lie within the cytoplasmic domain between transmembrane repeat III and repeat IV and within the repeat IV-S6 segment of the α-subunit Na^+ channels (Stühmer et al., 1989; West et al., 1992; McPhee et al., 1994). The III–IV linker may act as the inactivation particle and the IV-S6 segment as its receptor. This fast inactivation machinery appears to be analogous to the molecular mechanism found for the fast N-type inactivation of *Shaker* K^+ channels (Hoshi et al., 1990; Isacoff et al., 1991; Jan and Jan, 1992).

Besides fast inactivation, Na^+ channels are also subjected to slow inactivation when the membrane is depolarized for a prolonged period. Chandler and Meves (1970) described the slow inactivation process in squid axons, which takes several seconds to complete when the membrane is depolarized. Recovery from slow inactivation occurs when the membrane is repolarized. The time course of this recovery is also slow and may take several minutes. Rudy (1978) later found that slow inactivation remains intact when the fast inactivation process is destroyed by pronase treatment. Consistent with this finding, Wang and Wang (1996) showed that slow inactivation in cloned α-subunit rat muscle channels expressed in stable cell lines also remains functional when the fast inactivation process is eliminated by an oxidant, chloramine-T (CT). Recent studies on μ1-W402C (at the external flanking region of the I-S6 segment) and μ1-T698M (at the II-S5 segment) mutant rat muscle Na^+ channels show that slow inactivation can be completely or partially eliminated by mutation (Balser et al., 1996; Cummins and Sigworth, 1996). These results suggested that fast and slow inactivation are governed by separate molecular entities.

In an unrelated attempt to map the extent of the binding interactions between local anesthetics and their putative receptor in the IV-S6 domain of the Na^+ channel α-subunit (Ragsdale et al., 1994), we mutated the conserved asparagine (N) residue within the S6 transmembrane domain of all four repeats (see Diagram 1) in μ1 Na^+ channels (Trimmer et al., 1989).

Diagram 1.

μ1 Repeats	5	10	15	20	25
I-S6	YMIFF	VVIIF	LGSFY	LI**N**LI	LAVVA MAY
II-S6	CLTVF	LMVMV	IGNLV	VL**N**LF	LALLL SSF
III-S6	MYLYF	VIFII	FGSFF	TL**N**LF	IGVII DNF
IV-S6	GICFF	CSYII	ISFLI	VV**N**MY	IAIIL EN
Shaker S6 (ShB)	IVGSL	**CV**VAG	VLTIA	LPVPV	IV

Received for publication 15 August 1996 and in final form 7 January 1997.
Address reprint requests to Dr. Ging Kuo Wang, Department of Anesthesia, Brigham and Women's Hospital, 75 Francis Street, Boston, MA 02115. Tel.: 617-732-6879; Fax: 617-732-6927; E-mail: wang@zeus.bwh.harvard.edu.

0006-3495/97/04/1633/08 $2.00

The N residue is present in the 18th position of all S6 segments (underlined). There is no clear sequence homology between the *Shaker* S6 segment and the S6 segments of Na^+ channels. The CV residues (underlined) in the *Shaker* S6 segment are known to participate in C-type slow inactivation in tetrameric *Shaker* K^+ channels (Hoshi et al., 1991; Boland et al., 1994). Kinetically, C-type slow inactivation in *Shaker* K^+ channels resembles the slow inactivation in Na^+ channels. Unexpectedly, we found that the N (434)→A mutant in the I-S6 domain is highly sensitive to repetitive pulses, which elicit strong use-dependent inhibition of the mutant Na^+ current. In this report we focus on the current kinetics of N434A mutant channels and demonstrate that such a mutation in the I-S6 region of μ1 Na^+ channels alters slow inactivation drastically.

MATERIALS AND METHODS

Mutagenesis and transient transfection of HEK293t cells

The rat muscle μ1 cDNA (Trimmer et al., 1989) was cloned into the *Eco*RI site of a vector MT64 (Boylan and Gudas, 1991) to yield the plasmid μ1-MT64. Mutagenesis of μ1 was performed on μ1-MT64 by means of the Transformer Site-Directed Mutagenesis Kit (Clontech Lab., Palo Alto, CA), with some modifications to increase the yield of in vitro DNA synthesis. Two primers (a mutagenesis primer and a restriction primer) were used to generate the desired mutants. The restriction primer is 5′-GATCCTCTAGACTCGAGCTGCAGCCAA-3′, in which the wild-type *Sal*I site has been changed to a *Xho*I site (underlined). Primers for each S6 segment are as follows (Diagram 2), with the altered nucleotides underlined.

Diagram 2.

		Residue mutated
I-S6	CCTTCTACCTCATCGCT CTGATCCTGGC-3′	N434A
II-S6	CTGGTGGTCCTGGCTCTG TTCCTGGC-3′	N789A
III-S6	CCTTCTTCACCCTCGCCCT CTTCATCGG-3′	N1281A
IV-S6	CATCGTGGTCGCCATG TACATTGC-3′	N1584A

In vitro synthesis was performed for a total of 4 h, with one addition of NTPs and T4 DNA polymerase during the reaction. After digestion of DNA with *Sal*I to remove wild-type DNA, intact plasmids were transferred into mut-XL cells (Strategene cloning system, La Jolla, CA). The potential mutants were identified as *Sal*I-resistant and *Xho*I-containing plasmids. The mutation in the μ1-MT64 plasmid was confirmed by DNA sequencing. The cDNA of mutant μ1-MT64 was subcloned into a cDNA1/Amp vector (Invitrogen, San Diego, CA) for transfection experiments. To ascertain that no additional mismatch-mutation occurred in the N434A clone (N434A-1), we later isolated an independent clone (N434A-2) and found that this clone was indistinguishable from N434A-1 clone in our experiments.

The culture of HEK293t cells and their transient transfection with wild-type and mutant μ1 clones were undertaken as described by Cannon and Strittmatter (1993). Cells were grown to 50% confluence in a Ti25 flask and transfected by a calcium phosphate precipitation method. Transfection of μ1-pcDNA1 (10 μg) and reporter plasmid CD8-pih3m (1 μg) was satisfactory under these conditions. At 15 h after transfection, cells were trypsinized and replated to an appropriate density in 35-mm tissue culture dishes. Transfected cells were used for experiments as early as 4 h and as late as 3 days after replating. Transfection-positive cells were identified by CD8-DYNABEADS (Lake Success, NY) before current recording. Of the approximately 20–50% of cells that were CD8-positive, most cells expressed >1 nA Na^+ currents at +30 mV. Cells expressing <1 nA were not used to avoid the possible contamination of intrinsic Na^+ currents (usually <0.2 nA).

Electrophysiology and data acquisition

Conventional whole-cell recording techniques were used as previously described (Cota and Armstrong, 1989). Experiments were conducted under a reversed Na^+ gradient to minimize the series resistance artifact unless indicated otherwise. The holding potential was set at −100 mV. Data were obtained by EPC-7 amplifier (List Electronic, Dramstadt/Eberstadt, Germany), filtered at 3 KHz, and collected using pCLAMP software (Axon Instruments, Burlingame, CA). Patch electrodes contained either 100 mM NaF, 30 mM NaCl, 10 mM EGTA, and 10 mM HEPES adjusted to pH 7.2 with CsOH (130 mM Na^+ internal solution) or 10 mM NaCl, 120 mM CsF, 10 mM EGTA, and 10 mM HEPES adjusted to pH 7.2 with CsOH (10 mM Na^+ internal solution). The electrodes had a tip resistance of about 0.5–1.0 MΩ. The bath contained either 150 mM choline Cl, 0.2 mM $CdCl_2$, 2 mM $CaCl_2$, and 10 mM HEPES adjusted to pH 7.4 with tetramethyl hydroxide (0 mM Na^+ external solution) or 130 mM NaCl, 20 mM choline Cl, 0.2 mM $CdCl_2$, 2 mM $CaCl_2$, and 10 mM HEPES adjusted to pH 7.4 with tetramethyl hydroxide (130 mM Na^+ external solution). CT was purchased from Aldrich Chemical Company (Milwaukee, WI). It was freshly dissolved in external solution and used within 4–5 h. Treatment of CT was limited to <10 min. Liquid junction potentials were less than 3 mV and were not corrected. Series resistance errors on average were <4 mV after compensation. All experiments were performed at room temperature (23 ± 2°C).

Whole-cell data were analyzed by pCLAMP programs and displayed for curve fitting with the ORIGIN program (MicroCal, Northampton, MA). Leak and capacitance were subtracted by an analog device. No P/−4 subtraction (pCLAMP software) was used for the repetitive-pulse protocol. Data are presented as mean ± SEM values. An unpaired Student's *t*-test (SigmaStat, Jandel Scientific Software, San Rafael, CA) was used to evaluate the significance of changes in kinetic parameters. p values of <0.05 were considered statistically significant.

RESULTS

Rightward voltage shift in activation of N434A μ1 mutant channels

The voltage dependence of the activation of wild-type and N434A μ1 mutant Na^+ channels was characterized under a normal Na^+ gradient with a 130 mM external and a 10 mM internal Na^+ concentration. Fig. 1 *A* shows that wild-type μ1 Na^+ channels were activated by depolarization near a threshold of −50 to −40 mV, reached a maximum at −10 mV, and reversed from inward to outward at around +60 mV. In contrast, as shown in Fig. 1 *B*, mutant channels were activated near a threshold of −30 to −20 mV and reached a maximum at +10 mV. The reversal potential for mutant channels (63.1 ± 2.1 mV, n = 9, versus 65 mV predicted) remained nearly the same as that for the wild type (61.0 ± 1.8 mV, n = 5). The difference in the activation process became apparent when the normalized peak Na^+ current amplitude was plotted against the voltage (Fig. 1 *C*). The relative peak conductance was also calculated and plotted against voltage; the voltage corresponding to 50% of channel activation ($E_{0.5}$) was −24.0 ± 1.7 mV (n = 5) for the wild-type channels and −0.7 ± 1.3 mV (n = 9) for the

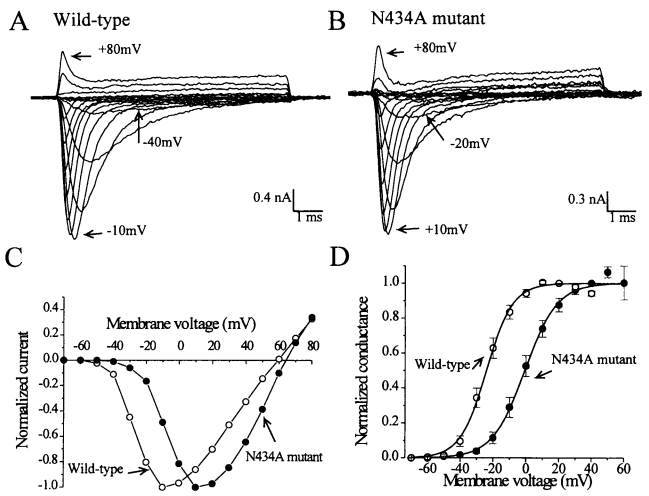

FIGURE 1 Activation of wild-type and mutant (N434A) μ1 Na^+ channels. Wild-type (*A*) and mutant N434A (*B*) μ1 Na^+ currents at various voltages were measured under a normal Na^+ gradient and superimposed. Noninactivating residual outward currents were evident at voltages higher than +30 mV; these currents were also present in untransfected HEK293t cells and were insensitive to tetrodotoxin. The peak current amplitudes in *A* and *B* were measured, normalized with respect to the maximum inward Na^+ current, and plotted against voltage as shown in *C*. The Na^+ conductance was then estimated by the equation $g = I_{Na}/(E - E_{rev})$, where I_{Na} is the peak current amplitude, E_{rev} is the estimated reversal potential, and E is the corresponding voltage. The results were normalized with respect to the measured values at +20 and +40 mV for wild-type and mutant channels, respectively (*D*). The data were least-squares fitted with a Boltzmann equation (*D*, *solid lines*): $y = 1/\{[1 + \exp(E_{0.5} - E)/k_a]\}$, where $E_{0.5}$ is the voltage at which $y = 0.5$ and k_a is the slope factor. Estimated values are listed in Table 1.

mutant channels (Fig. 1 *D* and Table 1). The slope of the activation process, as determined by the Boltzmann equation, was less steep for mutant than for wild-type channels (k_a = 8.0 ± 1.5 mV versus k_a = 9.8 ± 1.2 mV), but this difference was not statistically significant (Table 1). Evidently, the activation process is significantly right-shifted in mutant channels, demonstrating that N434A modifies the activation process of the Na^+ channel.

TABLE 1 Voltage dependence of activation, fast inactivation, and slow inactivation of wild-type μl Na^+ channels and N434A mutant channels

Parameters	Wild-type μl Na^+ channels	N434A mutant channels
$E_{0.5}$ (activation)	−24.0 ± 1.7 mV (n = 5)	−0.7 ± 1.3 mV (n = 9)*
k_a	8.0 ± 1.5 mV (n = 5)	9.7 ± 1.2 mV (n = 9)
$h_{0.5}$ (fast inactivation)	−78.4 ± 0.1 mV (n = 6)	−66.2 ± 0.2 mV (n = 10)*
k_h	7.7 ± 0.1 mV (n = 10	8.0 ± 0.2 mV (n = 10)
$s_{0.5}$ (slow inactivation)	−58.5 ± 0.5 mV (n = 9)	−70.6 ± 0.5 mV (n = 9)*
k_s	11.1 ± 0.5 mV (n = 9)	5.3 ± 0.4 mV (n = 9)*

Parameters of activation ($E_{0.5}$, k_a), fast inactivation ($h_{0.5}$, k_h), and slow inactivation ($s_{0.5}$, k_s) were estimated according to the Boltzmann equations described in Figs. 1 *D*, 3 *C*, and 7, respectively.

*$p < 0.05$ for wild-type versus mutant channels. No statistical differences were found for the values of k_a (p = 0.40) and k_h (p = 0.29) for wild-type versus mutant channels.

Altered fast inactivation in N434A μ1 mutant channels

The time constants (τ_f) of the fast-decaying phase of wild-type and mutant Na^+ currents at voltages greater than +20 mV were determined under a reversed Na^+ gradient (Fig. 2, *A* and *B*) as described previously by Cota and Armstrong (1989). According to these authors, the τ_f values at less than +20 mV do not truely reflect the fast inactivation, because the current activation phase overlaps significantly with the current decaying phase. The fast-decaying phase of wild-type and mutant Na^+ currents was least-squares fitted by a single exponential function, and the time constant was plotted against the voltage (Fig. 2 *C*). The time constants of N434A mutant at the voltage range of +20 mV to +80 mV declined from 0.33 ± 0.01 ms to 0.22 ± 0.01 ms (n = 6), which were significantly faster than that of wild-type Na^+ channels (ranging from 0.41 ± 0.04 ms at +20 mV to 0.39 ± 0.05 ms at +50 mV, n = 6; $p < 0.05$). The τ_f values for wild-type μ1 Na^+ channels are practically constant at this voltage range (from +20 to +80 mV), a phenomenon

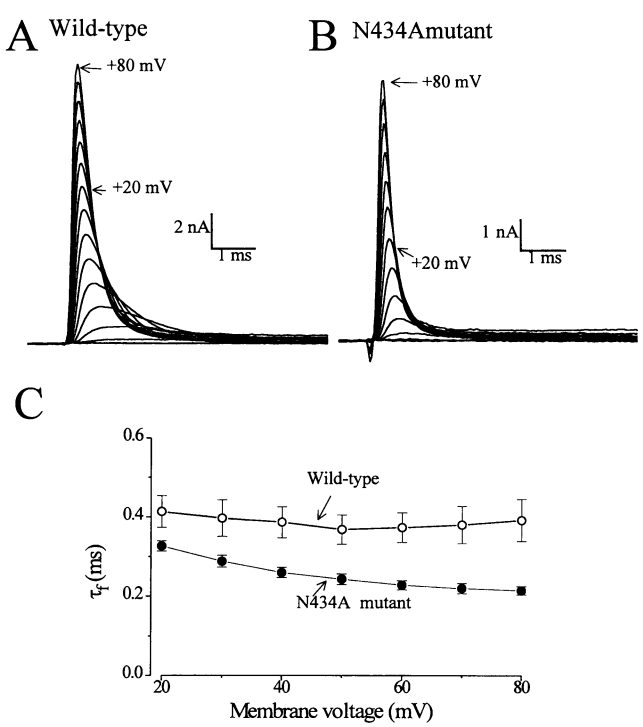

FIGURE 2 Fast inactivation of wild-type and mutant (N434A) μ1 Na^+ channels under a reversed Na^+ gradient. The fast-decaying Na^+ currents were activated by different voltages in steps of 10 mV and superimposed (*A* and *B*). The fast-decaying phase of Na^+ current was least-squares fitted by a single exponential function (τ_f) at voltages ≥ +20 mV. The τ_f values were then plotted against the corresponding voltage (*C*). The τ_f values for wild-type currents were significantly slower than those for N434A mutant currents (n = 6, $p < 0.05$).

also found previously for fast inactivation in GH_3 cells (Cota and Armstrong, 1989).

Steady-state inactivation of Na^+ channels was also measured under a reversed Na^+ gradient condition (Fig. 3, *A* and *B*) by the conventional two-pulse protocol (Hodgkin and Huxley, 1952). The $h_{0.5}$ values for wild-type and N434A mutant channels were measured at -78.4 ± 0.1 mV ($n = 6$) and -66.2 ± 0.2 mV ($n = 10$), respectively (Fig. 3 *C* and Table 1). These $h_{0.5}$ values of steady-state inactivation differed significantly ($p < 0.05$), whereas the slope factor values (k_h) did not (7.7 ± 0.1 mV, $n = 6$ for wild-type versus 8.0 ± 0.2 mV, $n = 10$ for N434A mutant; Table 1). These results together suggest that the fast inactivation process is also altered in mutant Na^+ channels.

Use-dependent inhibition of N434A μ1 mutant channels by repetitive pulses

Wild-type μ1 Na^+ channels appeared to be rather insensitive to repetitive pulses applied at 5 Hz with a duration of 25 ms; about 10% of peak currents in this cell were inhibited after 60 pulses (Fig. 4 *A*). In contrast, N434A mutant

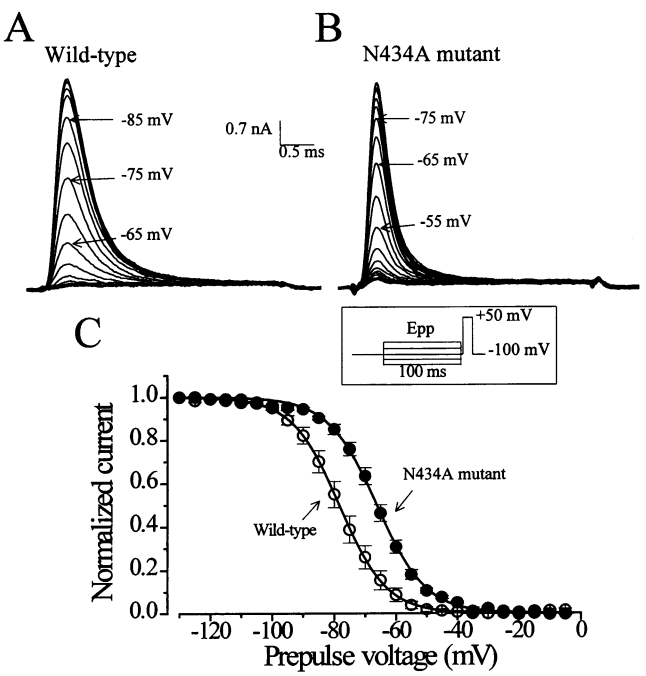

FIGURE 3 Steady-state inactivation of wild-type and mutant (N434A) μ1 Na^+ channels under a reversed Na^+ gradient. A two-pulse protocol was applied to measure the steady-state inactivation (Hodgkin and Huxley, 1952) with the prepulse potentials (E_{pp}) varying from -130 to -5 mV for 100 ms in steps of 5 mV (*A* and *B*). The numbers shown in the figure indicate the corresponding E_{pp} applied. The peak Na^+ currents for wild-type and mutant channels were measured at a contant test pulse of +50 mV, normalized with respect to the value measured at $E_{pp} = -130$ mV, and plotted against E_{pp} (*C*). A small residual noninactivating current was present and was subtracted before normalization. The data were least-squares fitted with a Boltzmann equation (*C*, *solid lines*): $y = 1/\{1 + \exp[(E_{pp} - E_{0.5})/k_h]\}$, where k_h is the slope factor and $E_{0.5}$ is the voltage at which $y = 0.5$. Estimated values are listed in Table 1.

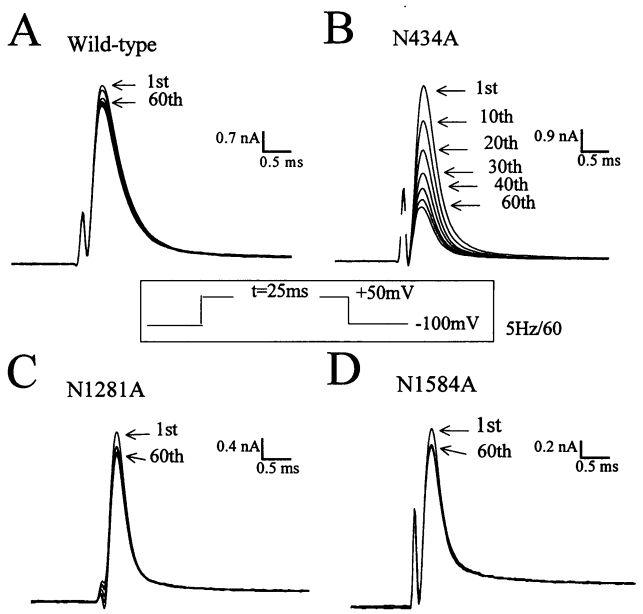

FIGURE 4 Use-dependent inhibition of wild-type and mutant μ1 Na^+ channels. Superimposed Na^+ current traces of wild-type (*A*) and mutant (*B–D*) channels were recorded during a repetitive-pulse protocol (*inset*). A profound use-dependent inhibition developed in mutant N434A but not in wild-type, N1281A, and N1584A mutant Na^+ channels. The numbers shown in the figure indicate the corresponding pulse number applied. Notice that the decaying phase of mutant channels is faster than that of wild-type channels. The expression of N1584A current was generally small compared to the expression of wild-type, N434A, and N1281A currents. Noninactivating TTX-insensitive residual outward currents of <0.4 nA were normally present at +50 mV.

channels were highly sensitive to the repetitive pulse, with more than 70% of currents inhibited by this protocol (Fig. 4 *B*). The time course of this use-dependent inhibition of peak Na^+ currents was least-squares fitted by a single exponential function with a time constant of 25.3 pulses (Fig. 5). The inward Na^+ current under a normal Na^+ gradient was as sensitive to repetitive pulses as the outward Na^+ current under a reversed Na^+ gradient, suggesting that external Na^+ ions have little effect on this use-dependent phenomenon (data not shown). Other N→A α-subunit mutants, N1281A and N1584A (Diagram 1) in repeats III and IV, respectively, did not display use-dependent inhibition of Na^+ currents similar to that exhibited by the N434A mutant (Fig. 4, *C* and *D*). The voltage dependence of the activation of N1281A and N1584A was also shifted rightward by about 10 and 20 mV, respectively. The fast-decaying phase of these two mutants was also significantly faster than the wild-type (Fig. 4 *A* versus 4 *C* and 4 *D*). The mutation in repeat II of N789A did not express Na^+ currents under our experimental conditions.

The duration of the repetitive pulses was important for the current inhibition of the N434A mutant: the longer the duration, the faster the rate and the higher the degree of use-dependent inhibition. For example, 86% of peak currents were blocked after 60 pulses at 5 Hz with a dura-

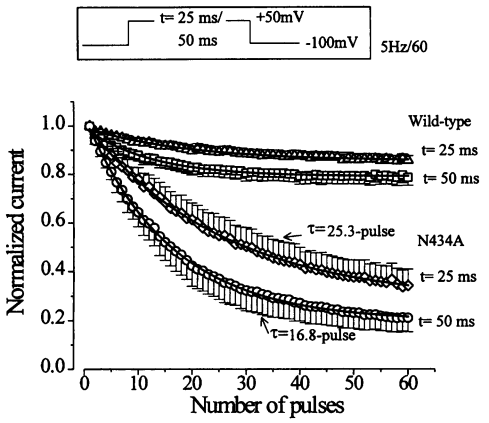

FIGURE 5 The rate of use-dependent inhibition of N434A mutant channels. The use-dependent inhibition of wild-type and N434A channels was determined by a pulse protocol shown in the inset. The duration of the pulse was set for either 25 or 50 ms. The peak current amplitude of each pulse was measured, normalized with respect to the amplitude of the first pulse, and plotted against the pulse number. Data (n = 5) were then least-squares fitted by a single exponential function (*solid lines*). Unlike N434A mutant currents, wild-type currents were relatively resistant to the use-dependent protocol; <20% of currents were inhibited, even with a 50-ms pulse duration. No correction was made for the small residual noninactivating outward currents.

tion of 50 ms. The rate of the current inhibition also varied, with a time constant of 25.3 pulses and 16.8 pulses for 25-ms and 50-ms duration, respectively. This result indicates that a cumulative depolarization of 1 s (50 ms/pulse × 16.8 pulses = 840 ms; Fig. 5) may be required for this use-dependent inhibition. Because of the relatively slow onset of use-dependent inhibition of Na^+ currents, we hypothesize that the slow inactivation of N434A mutant channels is altered.

Development of and recovery from slow inactivation of N434A mutant channels

To characterize slow inactivation, we applied a single conditioning pulse of +30 mV with a variable duration (t) and then measured the remaining peak current by a test pulse (Fig. 6 *A*, *inset*). Fig. 6 *A* shows that the slow inactivation measured at +30 mV developed over several seconds during the conditioning pulse, with a significantly longer time constant for wild-type channels than N434A mutant channels, i.e., 2.11 ± 0.10 s (n = 9) versus 0.46 ± 0.01 s (n = 9) ($p < 0.05$). The development of slow inactivation was voltage dependent in N434A mutant channels. The time constant for these mutant channels was estimated to be 1.5 ± 0.2 s (n = 3) at −30 mV, about threefold greater than the estimated value measured at +30 mV.

After N434A mutant channels entered their slow inactivated state by prolonged depolarization, recovery began with repolarization of the membrane to a holding potential of −100 mV. The time course of this recovery is shown in Fig. 6 *B*. The time course of recovery followed a single exponential function with a time constant of 115.8 ± 5.1 s (n = 6; Fig. 6 *B*, *solid circles*). In contrast, the time course of slow inactivation in wild-type channels (Fig. 3 *B*, *open circles*) was best fit by a two-exponential function with time constant values of τ_1 = 2.3 ± 0.3 s (46 ± 3%, n = 6) and τ_2 = 59 ± 6 s (46 ± 3%, n = 6). Most slow inactivated wild-type channels recovered and returned to their resting state sooner than their N434A counterparts.

Steady-state slow inactivation of N434A mutant channels

Steady-state slow inactivation (Fig. 7) can be measured by a pulse protocol (Chandler and Meves, 1970) similar to that

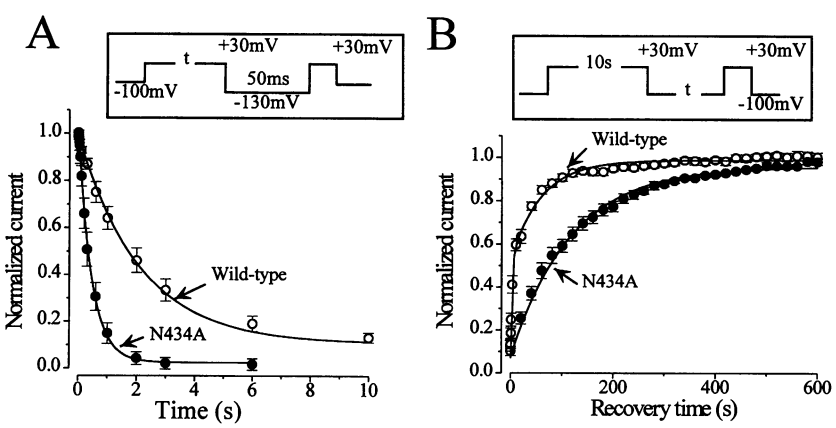

FIGURE 6 Development and recovery of slow inactivation in wild-type and mutant (N434A) μ1 Na^+ channels. (*A*) A single conditioning pulse at +30 mV with various durations (t) was applied to elicit slow inactivation, and the remaining Na^+ current was measured at a test pulse (see *inset*). An interpulse of −130 mV of 50 ms was inserted to allow the recovery of Na^+ channels from fast inactivation. Under identical experimental conditions, slow inactivation developed more slowly for wild-type channels than for mutant Na^+ channels. Data were least-squares fitted by a single exponential function (*solid lines*). (*B*) Recovery from slow inactivation was measured according to a pulse protocol shown in inset. Recovery from slow inactivation was faster for wild-type channels than for mutant channels. Data were least-squares fitted by either a single exponential function (mutant) or a two-exponential function (wild type).

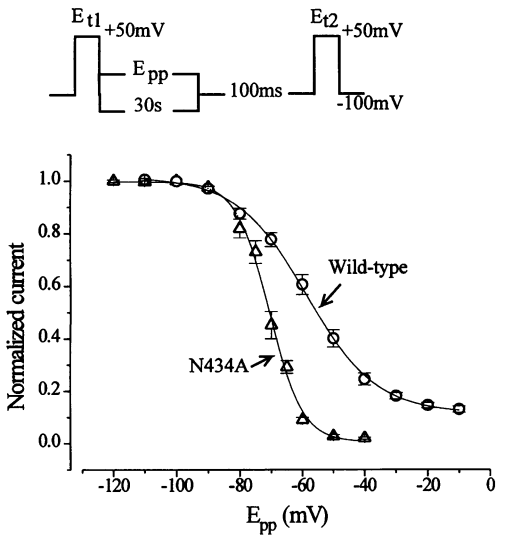

FIGURE 7 Steady-state slow inactivation of wild-type and mutant (N434A) μ1 Na^+ channels. Steady-state slow inactivation (s_∞) was measured by a three-pulse protocol (*inset*). Cells were allowed to rest at a holding potential of −100 mV for 360 s between pulses. The peak current amplitude was measured at E_{t2}, normalized with respect to the value measured at E_{t1} before each E_{pp}, and plotted against E_{pp}. The data were least-squares fitted with a Boltzmann equation: $y = 1/\{1 + \exp[(E_{pp} - E_{0.5})/k_s]\}$, where k_s is the slope factor, E_{pp} is the prepulse potential, and $E_{0.5}$ is the estimate of E_{pp} at $y = 0.5$. Estimated values are shown in Table 1.

used for the assessment of steady-state fast inactivation. The prepulse duration was set for 30 s, a period long enough to permit wild-type and mutant channels to enter their slow inactivated state at voltages near −70 mV. Fig. 7 shows the steady-state slow inactivation curve for wild-type and mutant channels. Unlike fast inactivation, the $s_{0.5}$ value of slow inactivation for mutant N434A (Table 1) was shifted toward the hyperpolarizing direction, and the slope was much steeper than that of the wild type. Slow inactivation of N434A reached its completion at −40 mV, whereas slow inactivation of the wild type remained incomplete, even at voltages near −10 mV (~10% of current remaining). A duration of 360 s at a holding potential of −100 mV for wild-type and mutant Na^+ channels was set between pulses. This duration was sufficiently long to ensure that most (>85%) of the slow inactivated Na^+ channels returned to their resting state before the next prepulse was applied. In addition, the peak currents measured at E_{t2} with a duration of 5 ms were renormalized to the peak currents measured at E_{t1} applied before the E_{pp} (Fig. 7). Table 1 lists the estimated parameters for the steady-state slow inactivation of wild-type and mutant N434A channels. This result suggests that the steady-state slow inactivation of mutant N434A is more sensitive to membrane voltage than is that of the wild-type. Together with Fig. 6, it is evident that N434A mutation promotes and stabilizes the slow inactivated state of μ1 Na^+ channels.

Direct observation of slow inactivation in N434A mutant

Fast inactivation of wild-type and mutant channels was readily abolished by treatment of external 0.5 mM CT for <10 min (Fig. 8, *A* and *B*). The peak current amplitude generally became larger after CT treatment; however, CT did not affect the voltage dependence or the kinetics of the activation process. With a slower time frame, slow inactivation of CT-modified wild-type and mutant channels could be directly visualized without using complicated pulse protocols (Fig. 8, *C* and *D*). The decaying phase of wild-type and mutant currents could be best fitted by a single exponential function with a time constant of 665 ± 50 ms and 208 ± 20 ms at +30 mV, respectively ($n = 6$). These time constants were severalfold faster than those measured with-

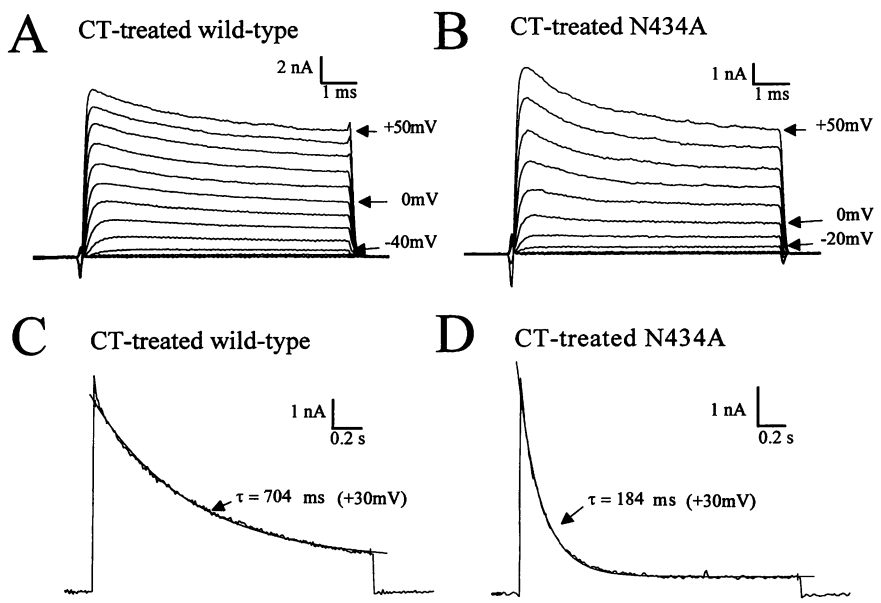

FIGURE 8 Fast and slow inactivation in CT-modified wild-type and mutant (N434A) μ1 Na^+ channels. After <10 min of external CT (0.5 mM) wash-in and subsequent washout, fast inactivation of wild-type (*A*) and mutant (*B*) μ1 Na^+ channels was nearly abolished. At this fast time frame, little inactivating currents remained at voltages from −40 to +50 mV; most currents were maintained at the end of an 8-ms pulse. There were no changes in the voltage dependence of activation or in the rising phase of CT-modified Na^+ channels. In contrast, slow inactivation was accelerated significantly in CT-modified wild-type (*C*) and mutant (*D*) μ1 Na^+ channels as shown in a slower time frame. The time course of this slow inactivation can be fitted by a single exponential with a time constant of 704 ms for wild-type and 184 ms for mutant channels (*fitted solid lines*). The small deviation from the fitted line for the first few milliseconds was probably due to residual unmodified Na^+ channels.

out CT treatment (Fig. 6 *A*), a finding that is consistent with a previous report on the slow inactivation of Na^+ channels in squid axons using pronase to remove fast inactivation (Rudy, 1978). Our results thus demonstrate that CT significantly accelerates the slow inactivation of wild-type and N434A mutant channels. However, the development of slow inactivation in CT-modified N434A mutant channels is still several times faster than that in CT-modified wild-type μ1 Na^+ channels, suggesting again that the N434 residue is critical for slow inactivation, even in the absence of fast inactivation.

DISCUSSION

Simultaneous alterations of fast and slow gating in mutant Na^+ channels

This report demonstrates that a mutation at N434 in segment I-S6 drastically alters the slow inactivation of μ1 α-subunit Na^+ channels. Additional results from pharmacological modifications of wild-type and mutant μ1 channels by CT further confirm that the residue of N434 is critical for the slow inactivation process. However, the mutant Na^+ channels also display significant changes in the voltage dependence of both activation and fast inactivation. These simultaneous modifications in fast and slow gating processes follow a single N→A substitution in position 434 of μ1 α-subunit Na^+ channels. How does a mutation at N434 affect not only the slow inactivation, but also the fast activation as well as the fast inactivation? The reason for this simultaneity in gating changes is not clear. The molecular structures involved in activation and fast inactivation of Na^+ channels have recently been investigated by site-directed mutagenesis (Stühmer et al., 1989; West et al., 1992; Yang et al., 1996). None of these studies has implicated any involvement of the I-S6 segment. Furthermore, the elimination of fast inactivation by CT in wild-type and mutant μ1 Na^+ channels also fails to eliminate slow inactivation. Instead, the development of slow inactivation is significantly accelerated severalfold in CT-modified Na^+ channels. Our result is consistent with a hypothesis that the open state of Na^+ channels can directly enter the slow inactivated state, but with a faster rate than the fast inactivated state can (for details see Rudy, 1978; Wang and Wang, 1996). Absolute coupling between fast and slow inactivation is therefore unlikely, because fast inactivation is not an obligatory step in the path to slow inactivation. However, it is possible that N434A mutation may cause decoupling of the partially coupled fast and slow inactivation processes in μ1 channels. Such a model would explain the acceleration of both fast and slow inactivation gating processes upon N434A mutation. Partial coupling of distinct gating regions has been suggested for the coupling of fast and slow inactivation in *Shaker* K^+ channels (Hoshi et al., 1991) and for the coupling of activation, fast inactivation, and slow inactivation in Na^+ channels (Bezanilla et al., 1982; Ruben et al., 1992; Balser et al., 1996).

Use-dependent block of mutant Na^+ channels

The most unforeseen result of the N434A mutation is the use-dependent behavior of the mutant Na^+ channels. Repetitive pulses of +50 mV at 5 Hz elicit significant use-dependent inhibition of mutant Na^+ channels. Wild-type μ1 Na^+ currents are quite resistant to such repetitive pulses, probably because slow inactivation develops much more slowly in wild-type Na^+ channels, with a time constant of 2.11 s. In contrast, mutant Na^+ channels enter their slow inactivated state rather rapidly, with a time constant of 0.46 s. The differences between wild-type and mutant Na^+ channels in terms of the development and recovery kinetics of slow inactivation suffice to explain the use-dependent phenotype in mutant Na^+ channels. In fact, profound use-dependent blocking phenomena can also be observed in CT-modified wild-type and mutant channels, because their development of slow inactivation is accelerated (data not shown). Could specific types in Na^+ channels display the use-dependent phenotype during repetitive pulses in vivo? In *Myxicola* axons, Na^+ currents, much like N434A mutant currents, decrease significantly during repetitive pulses, and the rate of decrease rises with the duration of pulsing (Rudy, 1981). Slow inactivation of Na^+ channels in *Myxicola* axons therefore functions as a frequency filter. This use-dependent phenomenon can explain various adaptation behaviors commonly documented in annelids. Whether other Na^+ channel types are greatly modulated by repetitive pulses in vivo remains to be seen. We have noticed that in a permanently transfected CHO-K1 cell line, slow inactivation of μ1 channels develops wtih a time constant of 3.0 ± 0.1 s (n = 11, Wang and Wang, 1996), significantly slower than the value reported here in transiently transfected cells under identical experimental conditions ($p < 0.05$). This difference implies that perhaps the lipid environment and/or the posttranslational modifications in these two cell lines may also modulate the kinetics of the slow inactivation.

"C-type" slow inactivation in mutant Na^+ channels?

Besides Na^+ channels, many types of voltage-gated ion channels are inactivated and recover with multiple exponential components; this observation suggests the existence of multiple inactivation processes. The fast and slow inactivation processes in *Shaker* K^+ channels have been well characterized and are called N-type and C-type inactivation, respectively. The differences in naturally occurring ShA and ShB variants in C-type inactivation are due to a single amino acid (valine at position 463; see Diagram 1) in the S6 segment (Hoshi et al., 1991). An adjacent mutation (at position C462A) of the *Shaker* K^+ channel has been found to accelerate C-type inactivation (Boland et al., 1994). Additional mutations at the S6 flanking region at the external mouth of the pore also modify the rate of C-type inactivation (Lopez-Barneo et al., 1993). As in *Shaker* variants, the kinetics of inactivation also differs considerably among

various types of voltage-gated Ca^{2+} channels. The differences of inactivation kinetics in Ca^{2+} channels are due to the different amino acid residues located in the I-S6 segment and in the extracellular and cytoplasmic domains flanking I-S6 (Zhang et al., 1994). It may not be a coincidence that the N434 residue in I-S6 of Na^+ channels is also important in governing the kinetics of slow inactivation. In fact, Zhang et al. (1994) suggested that Ca^{2+} and Na^+ channels may possess a similar form of C-type inactivation. Our results appear to confirm their prediction, but by no means exclude the involvement of other channel regions in slow inactivation. For example, μ1-T698M, a mutation located in the II-S5 region that causes episodes of hyperkalemic periodic paralysis at the equivalent human gene, has been reported to render slow inactivation incomplete in stable HEK-293 cell lines under normal Na^+ gradient (Cummins and Sigworth, 1996). In addition, Balser et al. (1996) recently reported that an external pore residue, W402C of μ1 channels, eliminates slow inactivation of Na^+ channels. The W402 position is at the external flanking region of I-S6 segment of μ1 channels. The phenotype found in these two mutants is the opposite of that of the N434A mutant. Clearly, further mutations in the I-S6 segment of Na^+ channels are needed to reveal the extent of its involvement in slow inactivation.

We are grateful to Dr. Stephen Cannon for providing the HEK293t cell line and the CD8-pih3m plasmid as a cotransfection marker, to Dr. Lorraine Gudas for the MT64 plasmid, and to Dr. James Trimmer for the pμ1–2 plasmid.

This work was supported by the National Institutes of Health (GM-35401 and GM-48090).

REFERENCES

Aldrich, R. W., D. P. Corey, and C. F. Stevens. 1983. A reinterpretation of mammalian sodium channel gating based on single channel recording. *Nature.* 306:436–441.

Armstrong, C. M. 1992. Voltage-dependent ion channels and their gating. *Physiol. Rev.* 72(Suppl.):S5–S13.

Balser, J. R., H. B. Nuss, N. Chiamvimonvat, M. T. Perez-Garcia, E. Marban, and G. F. Tomaselli. 1996. External pore residue mediates slow inactivation in μ1 rat skeletal muscle sodium channels. *J. Physiol. (Lond.).* 494:431–442.

Bezanilla, F., R. E. Taylor, and J. M. Fernandez. 1982. Distribution and kinetics of membrane dielectric polarization. 1. Long-term inactivation of gating currents. *J. Gen. Physiol.* 79:21–40.

Boland, L. M., M. E. Jurman, and G. Yellen. 1994. Cysteines in the Shaker K^+ channel are not essential for channel activity or zinc modulation. *Biophys. J.* 66:694–699.

Boylan, J. F., and L. J. Gudas. 1991. Overexpression of the cellular retinoic acid binding protein-I results in a reduction in differentiation-specific gene expression in F9 tetratocarcinoma cells. *J. Cell Biol.* 112:965–979.

Cannon, S. C., and S. M. Strittmatter. 1993. Functional expression of sodium channel mutations identified in families with periodic paralysis. *Neuron.* 10:317–326.

Catterall, W. A. 1988. Structure and function of voltage-sensitive ion channels. *Science.* 242:50–61.

Chandler, W. K., and H. Meves. 1970. Slow changes in membrane permeability and long-lasting action potentials in axons perfused with sodium fluoride. *J. Physiol. (Lond.).* 211:707–728.

Cota, G., and C. M. Armstrong. 1989. Sodium channel gating in clonal pituitary cells: the inactivation step is not voltage dependent. *J. Gen. Physiol.* 94:213–232.

Cummins, T. R., and F. J. Sigworth. 1996. Impaired slow inactivation in mutant sodium channels. *Biophys. J.* 71:227–236.

Hodgkin, A. L., and A. E. Huxley. 1952. A quantitative description of membrane current and its application to conduction and excitation in nerve. *J. Physiol. (Lond.).* 117:500–544.

Hoshi, T., W. N. Zagotta, and R. W. Aldrich. 1990. Biophysical and molecular mechanisms of *Shaker* potassium channel inactivation. *Science.* 250:533–538.

Hoshi, T., W. N. Zagotta, and R. W. Aldrich. 1991. Two types of inactivation in *Shaker* K^+ channels: effects of alterations in the carboxy-terminal region. *Neuron.* 7:547–556.

Isacoff, E. Y., Y. N. Jan, and L. Y. Jan. 1991. Putative receptor for the cytoplasmic inactivation gate in the *Shaker* K^+ channel. *Nature.* 353: 86–90.

Isom, L. L., K. S. DeJong, and W. A. Catterall. 1994. Auxiliary subunits of voltage-gated ion channels. *Neuron.* 12:1183–1194.

Jan, L. Y., and Y. N. Jan. 1992. Structural elements involved in specific K^+ channel functions. *Annu. Rev. Physiol.* 54:537–555.

Lopez-Barneo, J., T. Hoshi, S. H. Heinemann, and R. W. Aldrich. 1993. Effects of external cations and mutations in the pore region on C-type inactivation of Shaker potassium channels. *Receptors Channels.* 1:61–71.

McPhee, J. C., D. S. Ragsdale, T. Scheuer, and W. A. Catterall. 1994. A mutation in segment IVS6 disrupts fast inactivation of sodium channels. *Proc. Natl. Acad. Sci. USA.* 91:12346–12350.

Ragsdale, D. S., J. C. McPhee, T. Scheuer, and W. A. Catterall. 1994. Molecular determinants of state-dependent block of Na^+ channels by local anesthetics. *Science.* 265:1724–1728.

Ruben, P. C., J. G. Starkus, and M. D. Rayner. 1992. Steady-state availability of sodium channels: interactions between activation and slow inactivation. *Biophys. J.* 61:941–955.

Rudy, B. 1978. Slow inactivation of the sodium conductance in squid giant axons. Pronase resistance. *J. Physiol. (Lond.).* 283:1–21.

Rudy, B. 1981. Inactivation in *Myxicola* giant axons responsible for slow and accumulative adaptation phenomena. *J. Physiol. (Lond.).* 312: 531–549.

Stühmer, W., F. Conte, H. Suzuki, X. Wang, M. Noda, N. Yahagi, H. Kubo, and S. Numa. 1989. Structural parts involved in activation and inactivation of the sodium channel. *Nature.* 339:597–603.

Trimmer, J. S., S. S. Cooperman, S. A. Tomiko, J. Zhou, S. M. Crean, M. B. Boyle, R. G. Kallen, Z. Sheng, R. L. Barchi, F. J. Sigmworth, R. H. Goodman, W. S. Agnew, and G. Mandel. 1989. Primary structure and functional expression of a mammalian skeletal muscle sodium channel. *Neuron.* 3:33–49.

Wang, S-Y., and G. K. Wang. 1996. Slow inactivation of muscle u1 Na^+ channels in permanently transfected mammalian cells. *Pflugers Arch.* 432:692–699.

West, J. W., D. E. Patton, T. Scheuer, Y. Wang, A. L. Goldin, and W. A. Catterall. 1992. A cluster of hydrophobic amino acid residues required for fast Na^+ channel inactivation. *Proc. Natl. Acad. Sci. USA.* 89: 10910–10914.

Yang, N., A. L. George, and R. Horn. 1996. Molecular basis of charge movement in voltage-gated sodium channels. *Neuron.* 16:113–122.

Zhang, J., P. T. Ellinor, R. W. Aldrich, and R. W. Tsien. 1994. Molecular determinants of voltage-dependent inactivation in calcium channels. *Nature.* 372:97–100.